

Unbiased state reconstruction using modified weak measurement

Xuanmin Zhu^{1,*}, Yu-Xiang Zhang^{2,†} and Shengjun Wu^{3,‡}

¹ School of Physics and Optoelectronic Engineering, Xidian University, Xi'an 710071, China

²Hefei National Laboratory for Physical Sciences at Microscale,

University of Science and Technology of China, Hefei, Anhui 230026, China

³Kuang Yaming Honors School, Nanjing University, Nanjing, Jiangsu 210093, China

(Dated: December 8, 2024)

Based on the modified weak measurement scheme in [Y-X Zhang, S Wu and Z-B Chen, arXiv: 1504.07130], a modified direct state measurement (MDSM) is proposed without inherent bias. Compared with the existing direct state measurement (DSM), MDSM is more efficient and valid for any coupling strength. The optimal coupling strength used to attain the highest efficiency is given. With the same amount of samples, the precision of MDSM is less than the conventional QST, especially for higher dimensional systems. However, MDSM is much easier to be realized in actual experiments, and might be more useful.

PACS numbers: 03.67.-a, 03.65.Ta

I. INTRODUCTION

Though the quantum no-clone theorem prohibits the perfect estimation of an unknown quantum state from a single system [1, 2], state reconstruction is possible via repeated measurements on an ensemble of the identical state. There are two important state reconstruction strategies. One is the conventional quantum state tomography (QST) [3–10]; the other is called direct state measurement (DSM), by which the real and the image parts of the wave function could be measured directly [11–15]. Because of its directness and easier implementation in actual experiments, DSM has drawn much attention recently.

DSM is based on the concept of weak value which was introduced by Aharonov, Albert and Vaidman (AAV) in 1988 [16]. In DSM, by choosing the appropriate experimental variables, we can ensure that the element of the unknown density matrix is proportional to the weak value. In AAV's scheme, the necessary condition for obtaining weak values is the very weak coupling strength g between the unknown systems and measuring device [17–20]. Very weak coupling strength means little disturbance on the quantum systems and little information gain of the measuring device. Little information gain causes much lower efficiency of DSM [21]. In addition, DSM has an unavoidable error in the reconstructed state [21], due to the approximation applied in AAV's theory.

Recently, we have found that weak value information is unnecessary to be generated in AAV's weak measurement scheme. In Ref. [22], without any approximation, a new systemic scheme for pursuing weak value is proposed by measuring the coupling-deformed pointer observables. The new scheme is valid for arbitrarily large coupling

strength g . Therefore, the problems of the state reconstruction caused by weak interaction and approximation could be removed simultaneously. Particularly, the possibility of strengthening the measurements in DSM is also reported in Refs. [23, 24]. They have demonstrated that weak values are obtained by measuring three observables of measuring device.

Based on the new scheme for obtaining weak value in [22], a direct state reconstruction strategy named modified direct state measurement (MDSM) is studied. In MDSM, only two observables are measured, and the strategy is valid for arbitrary coupling strength g . In this paper, we give the optimal coupling strength g for attaining the highest efficiency. Through accurate Monte Carlo simulations, we compare the efficiency of MDSM with QST, and present the number of the copies needed in MDSM to attain the same reconstruction precision of QST.

This paper is organized as follows. In Sec. II we briefly review QST and DSM theories. MDSM is studied and the optimal coupling strength is given in Sec. III. Monte Carlo simulation results are given, and the efficiencies of different state reconstruction strategies are compared in section IV. A short conclusion is presented in Sec. V.

II. STRATEGIES FOR QUANTUM STATE RECONSTRUCTION

In this section, we briefly review the quantum state tomography, the direct state measurement with weak measurements, and present the modified direct state measurement.

A. quantum state tomography

Quantum state tomograph (QST) is a well-established state reconstruction technique without error bias. In QST theory [3], a quantum state ρ_{in} could be recon-

* zhuxuanmin2006@163.com

† iyxz@mail.ustc.edu.cn

‡ sjwu@nju.edu.cn

structed by

$$\rho_{in} = \int dg R^\dagger(g) \sum_i r_i^g \langle r_i^g | \rho_{in} | r_i^g \rangle, \quad (1)$$

where $R(g)$ is the unitary irreducible square-integrable representation of a tomographic group G , $g \in G$, $\{r_i^g\}$ is the orthonormal eigenvectors of $R(g)$, r_i^g is the eigenvalues of $|r_i^g\rangle$, and $\langle r_i^g | \rho | r_i^g \rangle$ is the probability of obtaining r_i^g . The derivation of Eq. (1) is given in [3]. As indicated by Eq. (1), a general unknown state ρ_{in} could be reconstructed by a series of measurements with the projective operators $\{|r_i^g\rangle\langle r_i^g|\}$. The tomographic group G used in this article is the SU(2) group, so we call this state reconstruction procedure *SU(2) tomography*. The detail of the strategy procedure is also in [3].

For qubit states, in addition to SU(2) tomography, there is a much more easily realized tomography named Pauli tomography [3]. In Pauli tomography, an unknown state can be expressed using the Pauli matrices

$$\rho = \frac{I}{2} + \sum_{i=x,y,z} \sigma_i \sum_{m_i=-1/2,1/2} \langle m_i | \rho | m_i \rangle, \quad (2)$$

where $\{|m_i\rangle\}$ is the orthonormal eigenvectors of the Pauli matrix σ_i . Just by measuring the three Pauli matrices, we could reconstruct an unknown two-dimensional state.

B. direct state measurement

The direct state measurement (DSM) is based on the weak measurement scheme. In DSM, to reconstruct an unknown state ρ_{in} , we firstly use a pointer in state $|\phi_0\rangle$ to weakly measure the system. The observables being measured are denoted as $\{A_i = |a_i\rangle\langle a_i|\}_i$. Therein, states in $\{|a_i\rangle\}_i$ compose an orthogonal basis of the system's Hilbert space. Secondly, we project the system onto states $\{|\psi_f\rangle\}_f$ which compose another orthogonal basis of the system's Hilbert space, which is usually called *post-selection*. We record the outcome of the post-selection and the readings of the pointer (with respect to the pointer observable denoted by \hat{s}). From the records, we can obtain the *weak value* of each A_i , which is defined as (when the system is post-selected to be $|\psi_f\rangle$)[13]

$$W_{if} = \frac{\langle \psi_f | a_i \rangle \langle a_i | \rho_{in} | \psi_f \rangle}{P_f}. \quad (3)$$

where P_f is the probability of obtaining the post-selected $|\psi_f\rangle$. For convenience, the measurement basis $\{|a_i\rangle\}_i$ and the post-selection basis $\{|\psi_f\rangle\}_f$ are always chosen to be the mutually unbiased bases (MUB) [25], which means $|\langle \psi_f | a_i \rangle| = 1/\sqrt{d}$.

We will relate weak values information to the measurements records in the below. After obtaining the set $\{W_{if}\}_{i,f}$, we could reconstruct the unknown state by the

formula

$$\rho_r = \sum_{i,f=1}^d \frac{P_f W_{if}}{\langle \psi_f | a_i \rangle} |a_i\rangle\langle \psi_f|. \quad (4)$$

The weak value is conventionally obtained via weak measurements with post-selection. In this article, the pointer is considered as a qubit initialized in a pure state $\rho_\phi = |0\rangle\langle 0|$, the eigenstate of σ_z : $\sigma_z|0\rangle = |0\rangle$. It couples to the system via the unitary

$$U_i(g) = \exp(-igA_i \otimes \sigma_x),$$

where A_i is the observable being measured, g is the tiny coupling strength. The real and imaginary parts of weak values are read out via two different pointer observables denoted as $\hat{s} \in \{\hat{q}, \hat{p}\}$, \hat{q} for the real part and \hat{p} for the imaginary part. Here the pointer is a qubit, we could choose

$$\hat{q} = \sigma_y, \quad \hat{p} = \sigma_x. \quad (5)$$

The weak value information required in DSM could be extracted from the weak measurements via

$$P_f W_{if} = \lim_{g \rightarrow 0} \frac{1}{2g} \text{tr}\{U_i(g)\rho_{in} \otimes \rho_\phi U_i^\dagger(g)\Pi_f \otimes (-\hat{q} + i\hat{p})\}. \quad (6)$$

The validity of Eq. (6) requires the weak limit. To get satisfied precision, we must employ a very tiny g , which implies little information gain [26] and low efficiency of DSM. The limit applied in Eq. (6) also implies that the error of the reconstruction is unavoidable, since an actual experiment must use a finite g . These two disadvantages of DSM have been presented by numerical simulations in [21]. In a recent work, without any approximation, a strategy is presented to pursue weak values by using *coupling-deformed* (CD) pointer observables [22]. We could use this strategy to propose a modified direct state measurement which is more efficient without inherent bias.

C. Modified direct state measurement

In Ref. [22], instead of the fixed pointer observables, \hat{s} is selected properly according to the coupling strength, and the weak value information can be exactly obtained. These pointer observables that depend on g are called coupling-deformed (CD) observables. Using the method in [22], we could calculate the corresponding CD pointer observables $\hat{q}(g)$ and $\hat{p}(g)$ in the state reconstruction strategy, which are

$$\begin{aligned} \hat{q}(g) &= \frac{g}{\sin g} \left(\sigma_y - \tan\left(\frac{g}{2}\right)(I - \sigma_z) \right); \\ \hat{p}(g) &= \frac{g}{\sin g} \sigma_x. \end{aligned} \quad (7)$$

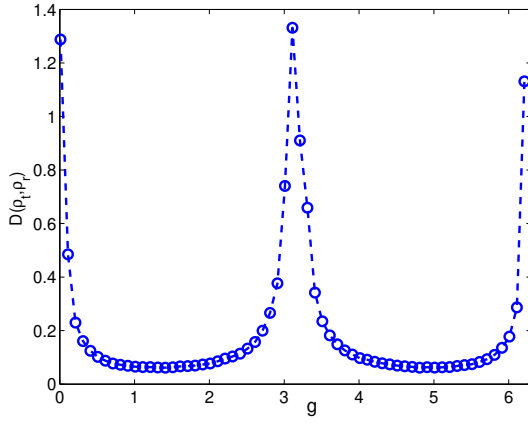


Figure 1. (Color online) The relationship between the trace distance and the coupling strength. D is averaged for 500 times repeated reconstructions.

Thus, the exact weak value is given by

$$P_f W_{if} = \frac{1}{2g} \text{tr}\{U_i(g)\rho_{in} \otimes U_i^\dagger(g)\Pi_f \otimes [-\hat{q}(g) + i\hat{p}(g)]\}. \quad (8)$$

Based on the values of $\{P_f W_{if}\}_{i,f}$ in Eq. (8), an unknown state could be reconstructed via Eq. (4). This new strategy is called modified direct state measurement (MDSM). Since there is no approximation used in MDSM. Hence, MDSM has no inherent bias, and valid for any g . A question arises naturally: which value of g should be chosen to gain the highest efficiency? In the next section, we will give the answer.

III. THE OPTIMAL MEASUREMENT STRENGTH

Firstly, we study the optimality by the standard Monte Carlo simulation: first, a value of g is fixed, and a general two-dimensional mixed state ρ_t is selected randomly as the target state with the number of the copies is 1000; second, the measurements (required by MDSM) implemented on the 1000 copies are simulated and results in an estimated state ρ_r ; third, the trace distance [27]

$$D(\rho_t, \rho_r) = \frac{\text{tr}(|\rho_t - \rho_r|)}{2} \quad (9)$$

between the true state ρ_t and the reconstructed state ρ_r is calculated to gauge the performance of MDSM. The less trace distance $D(\rho_t, \rho_r)$ means the higher efficiency of MDSM. For $g \in (0, 2\pi)$, in order to eliminate statistical fluctuations, we have averaged $D(\rho_t, \rho_r)$ for 500 times by the repeated reconstructions. As shown in Fig. 1, D attains its minimal value in the area $g \in [1, 1.6]$ or $g \in [4.7, 5.3]$.

In order to search for the optimal coupling strength more accurately, we have implemented further simula-

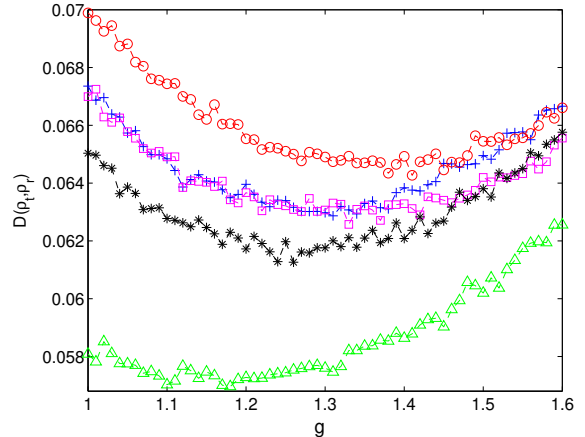


Figure 2. (Color online) The relationship between the trace distance and the coupling strength. D is averaged for 10000 times repeated reconstructions. Different symbols represent different unknown states.

tions. In these simulations, five randomly selected unknown mixed qubit states ρ_t are reconstructed with the 1000 copies. All the trace distances $D(\rho_t, \rho_r)$ are averaged for 10000 times in the area $g \in [1, 1.6]$. In Fig. 2, when $g \in [1, 1.6]$, the averaged $D(\rho_t, \rho_r)$ changes slightly, and could reach its minimal value. The smaller trace distance (higher precision of reconstruction) implies the higher efficiency. As indicated in Fig. 2, the optimal coupling strength is around $g = 1.3$.

Then, we investigate why the optimum is obtained around $g = 1.3$ in theory. The discrepancy between the true state ρ_t and the reconstructed state ρ_r comes from the statistical errors in the measurements. The statistical errors are usually quantified by variances. The reconstruction state ρ_r could be expanded as

$$\rho_r = \sum_{i,f=1}^d \varrho_{if} |a_i\rangle\langle\psi_f|.$$

In Eq. (4), we have $\varrho_{if} = P_f W_{if} / \langle\psi_f|a_i\rangle$ which is determined by the independent measurements. Therefore, the total variance of the reconstruction state ρ_r is

$$\delta^2 \rho_r = \sum_{i,f=1}^d \delta^2(\varrho_{if}). \quad (10)$$

As $|\langle\psi_f|a_i\rangle| = 1/\sqrt{d}$, using the error propagation theory [28], the total variance $\delta^2 \rho_r$ could be expressed as

$$\delta^2 \rho_r = d \sum_{i,f=1}^d \delta^2(P_f W_{if}). \quad (11)$$

From Eq. (8), we have

$$\begin{aligned} \delta^2 \rho_r = d \sum_{\hat{s} \in \{\hat{q}', \hat{p}'\}} \sum_{i,f=1}^d \text{tr}\{U_i \rho_t \otimes \rho_\phi U_i^\dagger \Pi_f \otimes \hat{s}^2(g)\} \\ - \left(\text{tr}\{U_i \rho_t \otimes \rho_\phi U_i^\dagger \Pi_f \otimes \hat{s}(g)\} \right)^2, \end{aligned} \quad (12)$$

where

$$\begin{aligned} \hat{q}'(g) &= \frac{1}{\sin(g)} [\sigma_y + \tan \frac{g}{2} (I - \sigma_z)], \\ \hat{p}'(g) &= \frac{1}{\sin(g)} \sigma_x. \end{aligned} \quad (13)$$

As shown in Eq. (8), $(\text{tr}\{U_i \rho_t \otimes \rho_\phi U_i^\dagger \Pi_f \otimes \hat{q}'(g)\})^2$ and $(\text{tr}\{U_i \rho_t \otimes \rho_\phi U_i^\dagger \Pi_f \otimes \hat{p}'(g)\})^2$ are the squares of the real and imaginary parts of $P_f W_{if}$ respectively. From Eq. (3), we find that $P_f W_{if}$ is independent of the coupling strength. As a result, the second term of Eq. (12) is independent of g .

Therefore, we just need to focus on the first term of $\delta^2 \rho_r$ in Eq. (12), which will be denoted as $TV1$. Using the relation that $\sum_f \Pi_f = I_s$, we have

$$TV1 = \sum_{\hat{s} \in \{\hat{p}', \hat{q}'\}} \sum_{i=1}^d \text{tr}\{\rho_i \hat{s}^2(g)\} \quad (14)$$

where $\rho_i = \text{tr}_s(U_i \rho_t \otimes \rho_\phi U_i^\dagger)$.

For $\hat{s}(g) = \hat{p}'(g)$, we have that $\hat{p}'(g)^2 = 1/\sin^2(g)$. Thus, we obtain

$$\text{tr}\{\rho_i \hat{p}'^2(g)\} = \frac{1}{\sin^2(g)}, \quad (15)$$

which is independent on the input state ρ_t . For $\hat{s}(g) = \hat{q}'(g)$, we have

$$\text{tr}_a\{\rho_i \hat{q}'^2(g)\} = \frac{1}{\sin^2 g} + 4c_i \tan \frac{g}{2} \cot g + 4c_i \tan^2 \frac{g}{2}, \quad (16)$$

where $c_i = \langle a_i | \rho_t | a_i \rangle$. Since $\sum_i c_i = 1$, $TV1$ is finally evaluated as

$$TV1 = \frac{2d}{\sin^2 g} + 4 \tan \frac{g}{2} \cot g + 4 \tan^2 \frac{g}{2}, \quad (17)$$

where d is the dimension of the unknown state.

In Fig. 3, the value of $TV1$ against the coupling strength $g \in [1, \pi/2]$ is illustrated for the dimension $d = 2$. For the area $g \in (0, \pi)$, the minimal value of $TV1$ locates at $g = 1.30$. As the second part of $\delta^2 \rho_r$ is independent of g , the total variance $\delta^2 \rho_r$ reaches its minimal value when $g = 1.30$. The smaller the value of $\delta^2 \rho_r$ is, the higher the efficiency of the tomography will be. Consequently, the optimal coupling strength is $g = 1.30$, which is consistent with the results in Fig. 2. The optimal coupling strength could also be obtained for higher

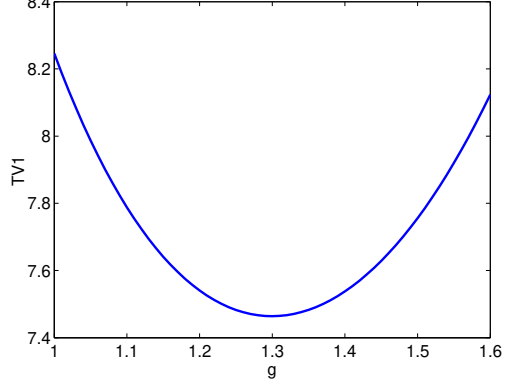


Figure 3. (Color online) The value of $TV1$ against the coupling strength g .

dimensions using Eq. (17). For example, the optimal coupling strength of MDSM is $g = 1.42$ for five dimensional states. Meanwhile, the expression diverges at the weak limit $g \rightarrow 0$. It verifies the conclusion that DSM at the weak limit suffers serious random noise, which causes its very low efficiency.

The exactness of the MDSM formalism, and its validity over the whole regime of measurement strength suggest that MDSM can overcome the problems of low efficiency and the intrinsic bias. In the next section, we will examine this claim by comparing the three strategies of quantum state reconstruction.

IV. COMPARISON

In this section, the efficiencies of MDSM, DSM, and QST are compared by Monte Carlo simulations. A two-dimensional state is reconstructed by MDSM, DSM, Pauli tomography and SU(2) tomography; and a five-dimensional state is reconstructed by MDSM, DSM and SU(2) tomography. The trace distance $D(\rho_t, \rho_r)$ between the true state ρ_t and the reconstructed state ρ_r is used to gauge the estimation efficiency.

As shown in Fig. 4, all the reconstruction strategies are affected by statistical errors. The trace distances decrease with the the numbers of the copies of the systems. As expected, the reconstructed state ρ_r of DSM has a bias; while the state ρ_r obtained by MDSM has no error bias. In MDSM, the trace distance $D(\rho_t, \rho_r)$ continues to decrease when the number of the copies increases.

For qubits, as indicated in Fig. 4, the efficiencies of MDSM, Pauli tomography and SU(2) tomography are close. In Fig. 5, for five-dimensional systems, the relationship between the trace distance and the number of the copies is given. Figure 5 indicates that although the MDSM has no bias, it is less efficient than SU(2) tomography for reconstructing a five-dimensional state. For the same reconstruction precision, MDSM need more copies than those in SU(2) tomography.

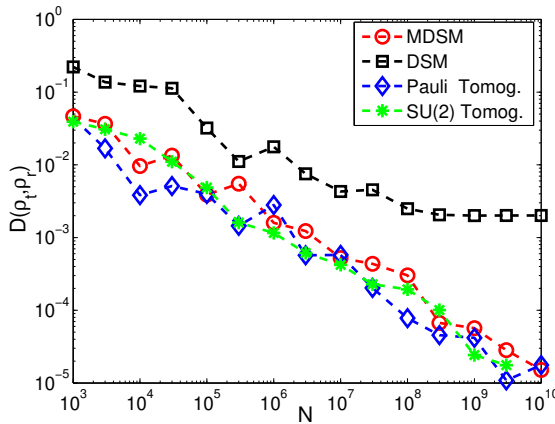


Figure 4. (Color online) Comparison between MDSM, DSM and QST for qubits. The trace distance $D(\rho_t, \rho_r)$ is plotted as the function of the numbers of copies N of the system. Circles, D calculated from MDSM with $g = 1.3$; squares, D calculated from DSM with $g = 0.1$; diamonds, D calculated from Pauli tomography; stars, D calculated from SU(2) tomography.

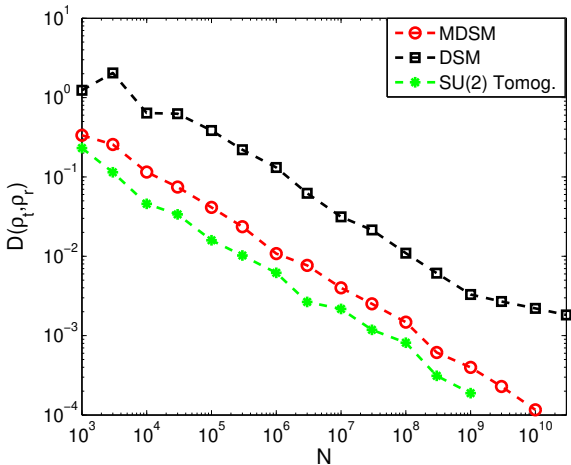


Figure 5. (Color online) Comparison between MDSM, DSM and QST for five-dimensional states. The trace distance $D(\rho_t, \rho_r)$ is plotted as the function of the numbers of copies N of the system. Circles, D calculated from MDSM with $g = 1.4$; squares, D calculated from DSM with $g = 0.1$; stars, D calculated from SU(2) tomography.

In order to study the gaps of the efficiencies between MDSM and SU(2) tomography, we have performed further simulations for two, four, five, six, eight, nine ten-dimensional systems. To achieve the same reconstruction precision, the numbers of copies needed for MDSM and SU(2) tomography are obtained respectively. The results of the simulations are listed on the tables of the appendix. The trace distances in the tables are averaged for 500 times repeated reconstructions to eliminate the statistical fluctuations.

As indicated in Tables I-III, MDSM needs the $0.8d$ times copies in SU(2) tomography to attain the same reconstruction precision for two, four and five-dimensional systems, where d is the dimension of the systems. In Tables IV-V, for six and eight-dimensional states, it is shown that MDSM need the $0.75d$ times copies of those in SU(2) tomography to attain the same precision. In Tables VI-VII, the $0.7d$ times copies are needed to attain the same precision for nine and ten-dimensional systems.

Roughly speaking, MDSM need the $0.8d$ times copies of the unknown quantum systems in SU(2) tomography to attain the same or a little better reconstruction precision for d dimensional systems. As conjectured, the reason of this conclusion is that only $1/d$ elements of the real (or image) part of the density matrix are obtained in each measurement of MDSM; while all the elements are obtained in each measurement of SU(2) tomography. Since SU(2) tomography needs measuring a complete set of non-commuting observables, which is difficult to be realized in actual experiments. Although MDSM is less efficient than SU(2) tomography, MDSM is much easier to be implemented in experiments. As a result, MDSM might be more useful than SU(2) tomography for reconstructing an unknown state, especially for high dimensional state.

V. CONCLUSION

We have presented a modified direct state measurement (MDSM) without inherent bias. MDSM is valid for any large coupling strength. The optimal coupling strength g to achieve the highest efficiency is given. MDSM is less efficient than SU(2) tomography especially for high dimensional state. We should need roughly $0.8d$ times copies of systems in SU(2) tomography to attain the same reconstruction precision. MDSM is much easier to be implemented in actual experiments, and it might be useful in reconstructing unknown quantum states.

ACKNOWLEDGMENTS

We thank Lorenzo Maccone for his helpful suggestions on SU(2) tomography. This work was financially supported by the National Natural Science Foundation of China (Grants No. 11305118, and No. 11475084), and the Fundamental Research Funds for the Central Universities.

VI. APPENDIX

In this appendix, we list seven tables to present the state reconstruction precision and the numbers needed in MDSM and SU(2) tomography respectively. All the trace distances are averaged for 500 times repeated reconstructions to eliminate statistical fluctuations.

MDSM	$N_1 = 1600$	$N_2 = 2560$	$N_3 = 4096$
$g = 1.3$	$D_1 = 0.0497$	$D_2 = 0.0386$	$D_3 = 0.0300$
SU(2)	$N'_1 = 1000$	$N'_2 = 1600$	$N'_3 = 2560$
tomography	$D'_1 = 0.0499$	$D'_2 = 0.0384$	$D'_3 = 0.0299$

Table I. The trace distances D (D') and the numbers N (N') of copies needed for two-dimensional systems in MDSM (SU(2) tomography).

MDSM	$N_1 = 3200$	$N_2 = 10240$	$N_3 = 32768$
$g = 1.4$	$D_1 = 0.140$	$D_2 = 0.0780$	$D_3 = 0.0435$
SU(2)	$N'_1 = 1000$	$N'_2 = 3200$	$N'_3 = 10240$
tomography	$D'_1 = 0.141$	$D'_2 = 0.0784$	$D'_3 = 0.0435$

Table II. The trace distances D (D') and the numbers N (N') of copies needed for four-dimensional systems in MDSM (SU(2) tomography).

MDSM	$N_1 = 4000$	$N_2 = 16000$	$N_3 = 64000$
$g = 1.4$	$D_1 = 0.192$	$D_2 = 0.0961$	$D_3 = 0.0481$
SU(2)	$N'_1 = 1000$	$N'_2 = 4000$	$N'_3 = 16000$
tomography	$D'_1 = 0.196$	$D'_2 = 0.0977$	$D'_3 = 0.0482$

Table III. The trace distances D (D') and the numbers N (N') of copies needed for five-dimensional systems in MDSM (SU(2) tomography).

MDSM	$N_1 = 9000$	$N_2 = 40500$	$N_3 = 182250$
$g = 1.4$	$D_1 = 0.182$	$D_2 = 0.0849$	$D_3 = 0.0404$
SU(2)	$N'_1 = 2000$	$N'_2 = 9000$	$N'_3 = 40500$
tomography	$D'_1 = 0.184$	$D'_2 = 0.0864$	$D'_3 = 0.0409$

Table IV. The trace distances D (D') and the numbers N (N') of copies needed for six-dimensional systems in MDSM (SU(2) tomography).

MDSM	$N_1 = 18000$	$N_2 = 108000$	$N_3 = 648000$
$g = 1.4$	$D_1 = 0.224$	$D_2 = 0.0916$	$D_3 = 0.0374$
SU(2)	$N'_1 = 3000$	$N'_2 = 18000$	$N'_3 = 108000$
tomography	$D'_1 = 0.233$	$D'_2 = 0.0954$	$D'_3 = 0.0390$

Table V. The trace distances D (D') and the numbers N (N') of copies needed for eight-dimensional systems in MDSM (SU(2) tomography).

MDSM	$N_1 = 31500$	$N_2 = 94500$	$N_3 = 315000$
$g = 1.4$	$D_1 = 0.211$	$D_2 = 0.123$	$D_3 = 0.0677$
SU(2)	$N'_1 = 5000$	$N'_2 = 15000$	$N'_3 = 50000$
tomography	$D'_1 = 0.214$	$D'_2 = 0.126$	$D'_3 = 0.0683$

Table VI. The trace distances D (D') and the numbers N (N') of copies needed for nine-dimensional systems in MDSM (SU(2) tomography).

MDSM	$N_1 = 21000$	$N_2 = 70000$	$N_3 = 210000$
$g = 1.4$	$D_1 = 0.316$	$D_2 = 0.175$	$D_3 = 0.100$
SU(2)	$N'_1 = 3000$	$N'_2 = 10000$	$N'_3 = 30000$
tomography	$D'_1 = 0.327$	$D'_2 = 0.180$	$D'_3 = 0.103$

Table VII. The trace distances D (D') and the numbers N (N') of copies needed for ten-dimensional systems in MDSM (SU(2) tomography).

[1] W. K. Wootters, W. H. Zurek, *Nature (London)* **299**, 802(1982).

[2] G. M. D'Ariano and H. P. Yuen, *Phys. Rev. Lett.* **76**, 2832 (1996).

[3] G. M. D'Ariano, L. Maccone, and M. Paini, *J. OPT. B: Quantum Semiclass. Opt.* **5**, 77 (2003).

[4] G. M. D'Ariano, L. Maccone, and M. G. A. Paris, *J. Phys. A* **34**, 93 (2001).

[5] D. F. V. James, P. G. Kwiat, W. J. Munro, and A. G. White, *Phys. Rev. A* **64**, 052312 (2001).

[6] A. E. Allahverdyan, R. Balian, and Th. M. Nieuwenhuizen, *Phys. Rev. Lett.* **92**, 120402 (2004).

[7] G. M. D'Ariano, L. Maccone, and M. F. Sacchi, in *Quantum information with Continuous Variables of Atoms and Light*, edited by N. Cerf, G. Leuchs, and E. Polzik (World Scientific Press, London, 2007).

[8] T. Durt, C. Kurtsiefer, A. Lamas-Linares, and A. Ling, *Phys. Rev. A* **78**, 042338 (2008).

[9] R. B. A. Adamson and A. M. Steinberg, *Phys. Rev. Lett.* **105**, 030406 (2010).

[10] H. Wang, W. Zheng, Y. Yu, M. Jiang, X. Peng, and J. Du, *Phys. Rev. A* **89**, 032103 (2014).

[11] J. S. Lundeen, B. Sutherland, A. Patel, C. Stewart, and C. Bamber, *Nature (London)* **474**, 188 (2011).

[12] H. F. Hofmann, *Phys. Rev. A* **81**, 012103 (2010).

[13] S. Wu, *Sci. Rep.* **3**, 1193 (2013).

[14] J. Z. Salvail, M. Agnew, A. S. Johnson, E. Bolduc, J. Leach, and R. W. Boyd, *Nat. Photon.* **7**, 316 (2013).

[15] Y. Shikano, in *Measurements in Quantum Mechanics*, edited by M. R. Pahlavani (InTech, Rijeka, 2012), p. 75.

[16] Y. Aharonov, D. Z. Albert, and L. Vaidman, *Phys. Rev. Lett.* **60** (1988) 1351.

[17] I. M. Duck, P. M. Stevenson, and E. C. G. Sudarshan, *Phys. Rev. D* **40**, 2112 (1989).

[18] R. Jozsa, *Phys. Rev. A* **76**, 044103 (2007).

[19] S. Wu and Y. Li, *Phys. Rev. A* **83**, 052106 (2011).

[20] X. Zhu, Y. Zhang, S. Pang, C. Qiao, Q. Liu, and S. Wu, *Phys. Rev. A* **84**, 052111 (2011).

[21] L. Maccone and C. C. Rusconi, *Phys. Rev. A* **89**, 022122 (2014).

[22] Y-X. Zhang, S. Wu, and Z-B. Chen, e-print arXiv:1504.07130 [quant-ph].

[23] G. Vallone and D. Dequal, e-print arXiv: 1504.06551 [quant-ph].

[24] P. Zou, Z-M. Zhang, and W. Song, *Phys. Rev. A* **91**, 052109 (2015).

[25] T. Durt, B. Englert, I. Bengtsson, and K. Zyczkowski, *Int. J. Quantum Inf.* **8**, 535 (2010).

[26] X. Zhu, Y. Zhang, Q. Liu, and S. Wu, *Phys. Rev. A* **85**, 042330 (2012).

[27] M. A. Nielsen, I. Chuang, in *Quantum Computation and Quantum Information*, (Cambridge University Press, Cambridge, 2000), p. 403.

[28] I. G. Hughes and T. P. A. Hase, in *Measurements and Their Uncertainties: A Practical Guide to Modern Error Analysis*, (Oxford University Press, New York, 2010), p. 38.